HOVERING FLIGHT OF THE DRAGONFLY AESCHNA JUNCEA L., KINEMATICS AND AERODYNAMICS

R. Åke Norberg

University of Göteborg

Göteborg, Sweden

ABSTRACT

The kinematics of free unimpeded hovering flight of Aeschna juncea L. was analysed from films taken in the field with 80 frames sec^{-1}, and from still pictures taken with a motorized camera.

The body is held almost horizontal, and the wing stroke plane is tilted 60° relative to the horizontal. In these respects the dragonfly differs strongly from most other hovering animals. The wing beats essentially in the same plane on the downstroke and upstroke. All wings are strongly supinated (pitched-up) during the upstroke. The stroke angle is ca. 60° and the wing beat frequency ca. 36 Hz.

Average, minimum force coefficients were calculated with use of steady-state aerodynamic theory. Calculations were made under several alternative assumptions and gave lift coefficients of 3.5 to 6.1, which are all far too large to be explainable with steady-state aerodynamics. At least 60% of the force generated in hovering flight are due to non-steady-state aerodynamics. The pitching rotations of the wings at top and bottom of the stroke are believed to contribute much force, although the exact mechanism is not clear.

At the leading edge of the wing of dragonflies there is a unique morphological arrangement, the node. It permits elastic tension of the leading edge and seems to be an adaptation permitting strong wing twistings. The node may also function as a shock absorber.

INTRODUCTION

Transient aerodynamic phenomena undoubtedly play some role in hovering flight of most insects. However, in most cases transient events need not be invoked to explain their hovering performance (Weis-Fogh (1973)).

The usual procedure to test this, and the one used in the present report, is to use wing and flight data and steady-state aerodynamic theory to make calculations of the aerodynamic forces necessary to sustain the insect (e. g. Osborne (1951) on ordinary flight; Weis-Fogh (1972) and (1973) on hovering flight). The crucial point is what magnitude of the force coefficients that is required to yield the necessary vertical force. If the calculations give a minimum average force coefficient, i. e. one giving just the necessary vertical force, that is smaller than the maximum force coefficient compatible with the wing shape and Reynolds number in question, then the flight performance is explainable with steady-state aerodynamics.

However, this is no proof that transient phenomena are not important. That result demonstrates only that transient phenomena need not be considered and that they may be of negligible importance. Weis-Fogh (1973) has shown that hovering flight of most types of insects are explainable with steady or quasi-steady aerodynamics. Although this is a sufficient explanation, it is not a necessary one, except when based on, and supported by detailed flight data. A more definite result (though more annoying) emerges when the hypothesis of steady-state aerodynamics is falsified. When the required minimum force coefficient arrived at is larger than the maximum one compatible with steady-state aerodynamics, then transient phenomena are bound to be important.

Weis-Fogh (1973) arrived at unreasonably large coefficients of lift, considering steady-state aerodynamics only, for hovering flight of four insect types. The insects were the chalcid wasp Encarsia formosa Gahan (Hymenoptera), with a wing length of ca. 0. 6 mm, the butterfly Pieris napi L. (Lepidoptera, Rhopalocera), the true hover-flies of subfamily Syrphinae, and two Aeschna dragonflies (Odonata).

Hovering flight of the true hover-flies and of dragonflies is remarkable in that these insects keep the long body axis about horizontal, have a very large angle of tilt of the wing beat plane, and beat the wings through relatively very small stroke angles. When hovering, most other insects have an upright body attitude and beat the wings in planes or figures of ∞ close to the horizontal.

Regarding Odonata, Weis-Fogh (1973, p. 206) wrote "...calculations...for Aeshna juncea (based on Sotavalta (1947)) and for Aeshna grandis (Weis-Fogh (1967)) show that hovering dragonflies must rely on non-steady aerodynamics because in both species each of the four wings should operate with a minimum $\overline{C}_L$ of 2.3." Apparently data from free hovering flight were not available (p. 181). Further, the induced velocity and angle of tilt of the stroke plane were not considered in the calculations that were aimed primarily at being simple.

The purpose of the present investigation is to describe the motions of the wings during free hovering flight of Aeschna juncea L. as analysed from films and still pictures taken in the field. Further, force coefficients are calculated with aid of equations devised by Weis-Fogh (1972), taking into account induced air velocity and angle of tilt of the stroke plane. Additional equations are given to account for tilts of the aerodynamic forces.

METHODS

Filming and Photographing

I know of no way of persuading dragonflies to hover freely in the laboratory. Therefore I filmed and photographed them in the field (in July and August in southwestern Sweden). The dragonfly Aeschna juncea often patrols back and forth along shore lines at heights of less than 1.5 m. It frequently stops and hovers for several seconds. From hovering flight it often accelerates rapidly in pursuit of some insect prey that it has detected while hovering.

Some films were taken at a tarn while most films and all photographs were taken at a pond, only ca. 20 m across. Filming and photographing were much easier at the pond, where the flight behaviour of the dragonflies was more predictable than at the larger tarn.

All films and still pictures were taken on sunny days with temperatures of about 20°C and with no aid of artificial light. Very weak winds sometimes did prevail during filming. Different film sequences are on dragonflies hovering in different orientations relative to the weak wind. No differences in the flight parameters used for calculations could be traced for the various situations, nor for different specimens. Updraughts are unlikely to have occurred (as judged from the drift of small insects and plumed seeds). Since the results are so similar for different specimens and conditions, horizontal and vertical winds seem not to have imposed any significant errors on the data used.

I used a Pathe Reflex BTL 16 mm film camera with a 50 mm lens and an exposure frequency of 80 frames sec^{-1}. The exposure frequency was checked by filming a stop watch and deviated less than 1.5% from 80 frames sec^{-1}. Ektachrome EF film and exposure times of 1/200-1/600 sec were used. Still pictures were taken at rates of 3-4 sec^{-1} using a motorized Leicaflex (SL MOT) 35 mm camera. It was equipped with a Telyt 1:6.8/400 mm lens with a rapid focusing device plus a 50 mm extension tube. Kodak Tri-X film and exposure time of 1/1000-1/2000 sec were used.

Analysis of the Films

The films were used to measure (1) wing beat frequency, (2) angle of tilt of the stroke plane, (3) wing beat angle, to (4) trace wing tip paths, and to (5) map attitudes and relative movements of fore- and hindwing.

At 80 frames sec^{-1} only two exposures were obtained per wing beat. The procedure used in analysis therefore was to project the film, frame by frame, onto a paper and mark out the position of the wing tips relative to the body. From the attitude of forewings and hindwings it could be determined whether a wing was moving up or down. This was also marked out on the plot. Tracing was continued until a frame turned up showing the wings in the same positions as in the first frame traced. Thereafter the number of wing beats covered was found. Combination with the exposure frequency gave the wing beat frequency as averaged over a number of wing beats (usually 4-6). This was done with film sequences both from the side and from in front.

The angle of tilt of the stroke plane can be read easily from the diagrams. Since only two exposures were obtained per wing beat, all 170 frames of one sequence (Figure 4) taken from in front, normal to the beat plane to within 5°, were looked at in search of ones showing the wings in extreme positions. Those frames were selected and used for measurement of beat angle. The true extreme positions may be missing from the film, but since so many frames were looked through, the underestimation should be negligible. The approximate wing tip path, as averaged over several consecutive wing beats, emerges from the composite plots (Figure 3).

From the film sequence taken from in front (see above) different phases were selected and drawn. After a number of frames a particular phase was found again, showing the wings in almost exactly the same attitudes. The pattern of wing movement thus seemed to be consistent in this sequence. I therefore felt

justified to select 12 pictures representing different phases and order them according to phase (Figure 4), and base the description of wing movements partly on this series. The pictures are from several wing strokes.

The still pictures (Figures 5-8) gave better resolution than did the 16 mm film, and supply further information on wing attitudes in various phases of the stroke.

Calculation of Force Coefficients

A hovering animal accelerates air downwards, the change of momentum furnishing the required upward force that must equal the weight. The movement of the accelerated air is assumed to be vertically downwards. Although the wings sweep through small sectors only, the horizontal projections of which are still smaller, it is assumed that the velocity imparted to the air is uniformly distributed over a 360° disc with diameter equal to the wing span, a course taken also by Pennycuick (1968) and Weis-Fogh (1972). In helicopter theory it is customary to assume that the volume of air accelerated by the rotor in hovering as well as in translatory flight, is equal to the volume passing through a sphere with the rotor span as diameter (Shapiro (1955)). This is the justification for the analogous assumption made here. This is one limiting case as to induced flow and gives minimum values of induced velocity and induced power. The other limiting case is if air is accelerated through only the horizontally projected area of the sectors actually swept by the wings. This alternative assumption would give maximum values of induced velocity and induced power. It is considered further in the section on Results. The induced velocity V_{ind} is estimated with aid of the momentum theory

$$V_{ind} = (W/2\rho A)^{\frac{1}{2}} \qquad (1)$$

where W is weight of the animal, ρ is density of air (1.22 kgm^{-3}) and A is area through which air is accelerated.

To simplify calculations, it is assumed that the wingstroke of the dragonfly in hovering flight is sinusoidal with respect to angular displacement, i.e. the wings are assumed to beat in simple harmonic motion.

The following method of calculation is adopted from Weis-Fogh (1972), and his equations are given below, slightly changed but the same in principle, and with some additional explanations.

Because of the large angle of tilt of the wing stroke plane in dragonflies, I give some additional equations (12, 13 and 14) for calculation of the vertical projection of the aerodynamic force.

The equation of angular movement (for simple harmonic motion) is

$$\gamma = \frac{1}{2}\phi \sin(2\pi ft) \qquad (2)$$

where γ is the instantaneous positional angle of the long wing-axis measured in the stroke plane and relative to the middle (mean) position of the wing. ϕ is the angle between the extreme positions of the wing, i.e. the stroke angle measured in the stroke plane, the amplitude being half the stroke angle, or $\frac{1}{2}\phi$. If the middle position of the wing is at angle ϵ, measured in the stroke plane and relative to the anteroventral intersection of the stroke plane with a sagittal plane (to the body) through the wing hinge (Figure 2), then the instantaneous positional angle α relative to the horizontal becomes

$$\alpha = \epsilon + \gamma - \frac{\pi}{2} \qquad (3)$$

In the calculations performed here, the middle position of the wing is taken to be on the horizontal plane, i.e. ϵ is taken to be 90° and thus α becomes equal to γ.

The angular velocity is

$$\frac{d\gamma}{dt} = \dot{\gamma} = 2\pi f \frac{1}{2}\phi \cos(2\pi ft) = \pi f \phi \cos(2\pi ft) \qquad (4)$$

where f is the wing stroke frequency, t is time, $2\pi f$ is the angular frequency (ω), and $\frac{1}{2}\phi$ is the amplitude. The tangential, flapping velocity V_r of a wing strip a distance r from the wing base is

$$V_r = r\dot{\gamma} = r\pi f \phi \cos(2\pi ft) \qquad (5)$$

The resultant relative air velocity $V_{res,r}$ is found by vector addition of the induced velocity and flapping velocity. The following equation is found from Figure 1 with aid of the cosine theorem

$$V^2_{res,r} = V^2_r + V^2_{ind} - 2V_r V_{ind} \cos(\frac{\pi}{2} - \beta) \qquad (6)$$

where β is the angle of tilt of the stroke plane relative to the horizontal. Actually, V_{ind} should be projected onto a plane

normal to the long wing-axis in analogy to the case of equation (14), and this component should be added vectorially to V_r to yield $V_{res,r}$. Since V_{ind} is small relative to V_r this projection was omitted.

The angle $$\psi = \beta - \delta \,, \tag{7}$$

and δ can be obtained from the following equation which follows from Figure 1

$$A = V_{res} \sin \delta = V_{ind} \cos \beta \tag{8}$$

The resultant aerodynamic force F_r on a chordwise wing strip with aera A_r is

$$F_r = \frac{1}{2} \rho V_{res,r}^2 A_r (C_L^2 + C_D^2)^{\frac{1}{2}} \tag{9}$$

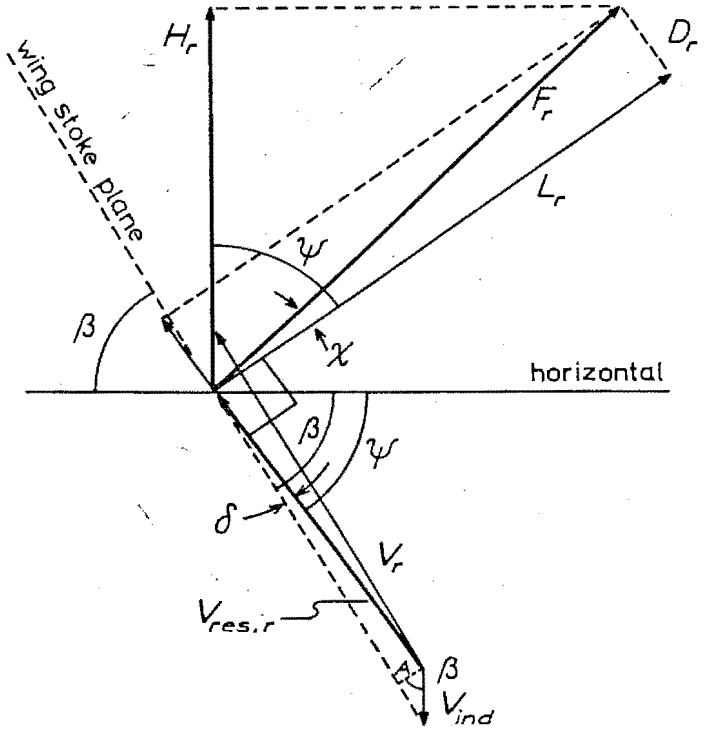

Figure 1. Relative air velocities and forces at a wing element a distance r from the wing base. All velocity and force vectors lie in a plane normal to the long wing-axis. The relative magnitudes of the air velocities are as calculated for a forewing element 75% of the wing length from the base and in the middle of the downstroke. The lift/drag ratio is taken to be 6.5

where C_L and C_D are lift and drag coefficients, respectively. From Figure 1 where L_r is proportional to C_L and F_r to the total force coefficient $(C_L^2 + C_D^2)^{\frac{1}{2}}$, it is seen that

$$(C_L^2 + C_D^2)^{\frac{1}{2}} = C_L/\cos\chi \tag{10}$$

Projection of the resultant aerodynamic force F_r on a vertical plane through the long wing-axis yields the force component H_r, which is normal to the long wing-axis (Figures 1 and 2)

$$H_r = \frac{1}{2}\rho V_{res,r}^2 A_r C_L \cos(\psi - \chi)/\cos\chi \tag{11}$$

The vertical projection $H_{r,vert}$ of H_r is

$$H_{r,vert} = H_r \cos\alpha_{proj} \tag{12}$$

where α_{proj} is the projection of angle α on a vertical plane through the long wing-axis. From the geometry of Figure 2 it is seen that

$$\begin{aligned}\cos\alpha_{proj} &= [r^2 - (r\sin\alpha\sin\beta)^2]^{\frac{1}{2}}/r \\ &= (1 - \sin^2\alpha\sin^2\beta)^{\frac{1}{2}}\end{aligned} \tag{13}$$

Combination of equations (12) and (13) gives

$$H_{r,vert} = H_r(1 - \sin^2\alpha\sin^2\beta)^{\frac{1}{2}} \tag{14}$$

In this case, where α_{max} is equal to 30° and β to 60°, the projection expressed in equation (14) affects (increases) the value of the calculated force coefficients by about 3.5% only.

Next, the forces must be integrated over the whole wings and averaged over a whole wing stroke cycle. Integration of forces over the wings was performed with aid of strip analysis. Averaging of forces with respect to time involves integration with respect to time and subsequent division by that time. Practically, however, this was done with aid of strip analysis for various times. To this end, the forewing was divided in 10 chordwise strips and their areas and the distance from middle of strip to wing base measured. Then the vertical force on each strip should be calculated for various time (i.e. various stroke phases) with equations

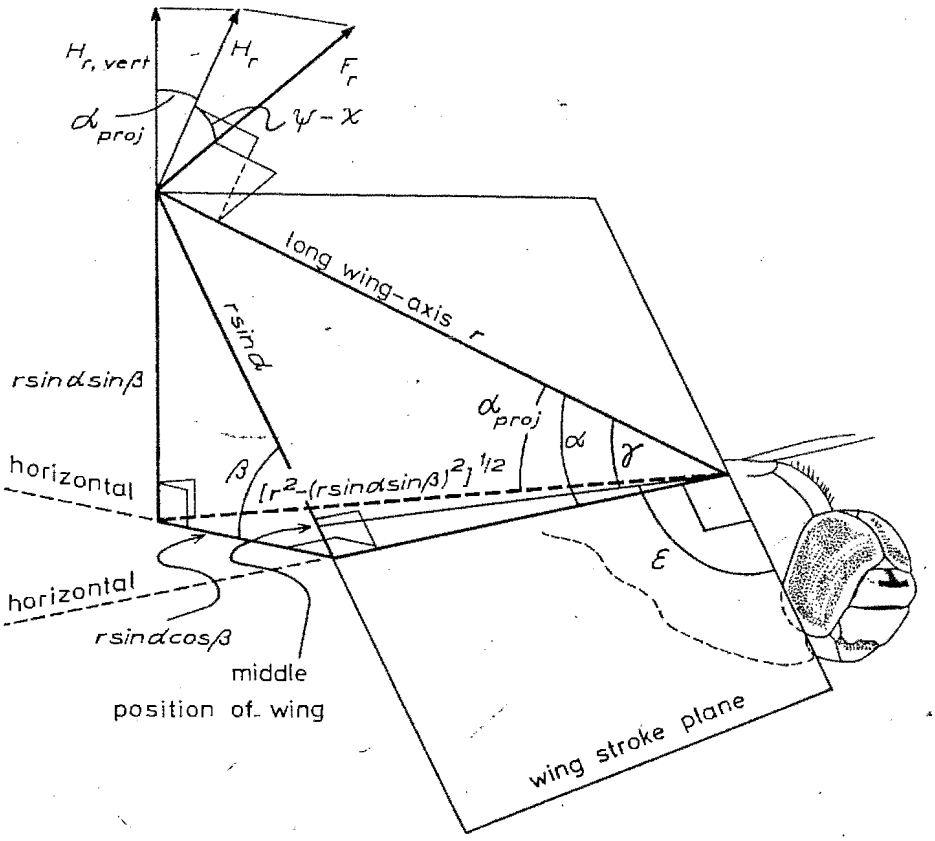

Figure 2. Diagram showing how the vertical projection $H_{r,\,vert}$ of the resultant aerodynamic force F_r is related to positional angle α of the wing and angle of tilt β of the stroke plane. See text for further explanation.

(11) and (14). However, since the force coefficients needed for this are the unknowns sought, they are omitted from the calculations to begin with. With aid of equations (11) and (14) I calculated a vertical pressure index $H_{r,\,vert}\cos\chi/C_L$ which is equal to $H_{r,\,vert}/(C_L^2 + C_D^2)^{\frac{1}{2}}$ (from equation (10)). Since the force coefficients are dimensionless, the index retains the dimension Newton. The pressure index for each of the ten strips was calculated at seven time-equidistant points over half a downstroke, the other half being identical. For each of the seven times, the pressure indices of all ten strips were added and plotted against time. Diagrams of this type appear in Figure 4 in Weis-Fogh (1972) and Figure 8 in U. M. Norberg (1974). For the most proximal strips the force is directed downwards due to the induced wind. Because of the low relative air velocity these forces are relatively very small and hence were disregarded as were those at the turning points.

The time-averaged value (for one whole wing stroke) of the vertical forces of all four wings must equal the weight of the dragonfly. That is, the force coefficients must be as large as to make the average vertical force equal to the weight. The value of the force coefficient was found graphically as follows.

Various assumptions were made regarding the force contribution during the upstroke (see below). For the case that the upstroke contributes no vertical force, the area was found under the curve for half a downstroke, and indicating the vertical pressure index versus time. Since the other half of the downstroke contributes as much force, but the upstroke none (under the assumption made), and since there are four wings, this area was multiplied with eight. The area of the hindwing is larger than that of the forewing. But the additional area of the hindwing is mainly from its proximal parts, where the relative air velocity and hence pressure are small. The hindwing therefore contributes only slightly more force than does the forewing. Then the area was found under the weight curve for the time of a whole wing beat cycle, i.e. under a horizontal line at a height indicating the weight of the dragonfly. This area was then multiplied by $\cos\chi$ and divided by the area representing the pressure index for all wings. The quotient arrived at is the C_L value sought. This coefficient is an average and a minimum one. Hence there are both larger and smaller values of the coefficient at various locales of the wing and at various times depending on different angles of attack.

Data on body mass, wing span, distance from middle of strip to wing base, and wing strip area used in calculations, all are from one male dragonfly, and were taken or measured from Norberg (1972, p. 12-13). I have no flight data for that specimen. The flight data used are those reported here from films of dragonflies in free hovering flight.

Hertel (1966, p. 25) gave a C_L/C_D ratio of 6.5 for the blue dragonfly, identified as Aeschna cyanea on his p. 78. Judging from the context, it is for an isolated wing. I use this value here for A. juncea which is very similar to A. cyanea. Support for such high C_L/C_D ratios for insect wings of this shape and size is found in Jensen (1956, p. 530), who obtained the ratio 5.7 at $C_{L,max}$ for the forewing of the locust Schistocerca gregaria Forskål.

RESULTS

The Wing Stroke

In hovering as well as in forward flight the body is kept horizontal or slightly inclined head-down. In nine film sequences on hovering flight head-down inclinations of the body were 0-6° with 2° as average value.

Wing beat frequencies from three film sequences on three specimens were 36, 36 and 37 Hz. Angle of tilt of the stroke plane relative to the horizontal was measured on 13 plots of wing tip paths for three specimens, giving an average of 59.8° (standard deviation 3). The wing beat angle was measured from one film sequence and was 60°. (Less accurate measurements from other sequences gave similar values.) In Figure 4 the forewing beats from 35° above the horizontal to 25° below, while the hindwing beats from 45° above to 15° below. In another sequence (Figure 3), however, the top position of the forewing is higher than that of the hindwing, which here beats through a smaller angle. The wings beat in essentially the same plane on the downstroke and upstroke.

The stroke of the forewing is as follows. From its top position the wing beats downwards with the chord almost horizontal (Figures 4 and 5). At bottom of the stroke the wing is strongly supinated, i.e. rotated in the nose-up sense, and twisted (Figures 4 and 7). During the upstroke the wing remains twisted and strongly supinated, with the chord close to the vertical (Figures 4, 7, and 8). At top of the stroke there is a pronation, i.e. a nose-down rotation that brings the chord back close to a horizontal position. This pronation is completed first at the wing tip (Figure 4:12).

The stroke of the hindwing is similar to that of the forewing. Supination of the hindwing at bottom of the stroke is completed first at the base (Figures 4:11, 4:12, and 4:1). During the upstroke the chord of the hindwing is close to the vertical also at the base (Figure 7). Pronation of the hindwing at top of the stroke is completed first at the tip (Figure 4:8), just as with the forewing (Figure 4:12).

The hindwing leads in phase by almost 180° (Figures 3 and 4).

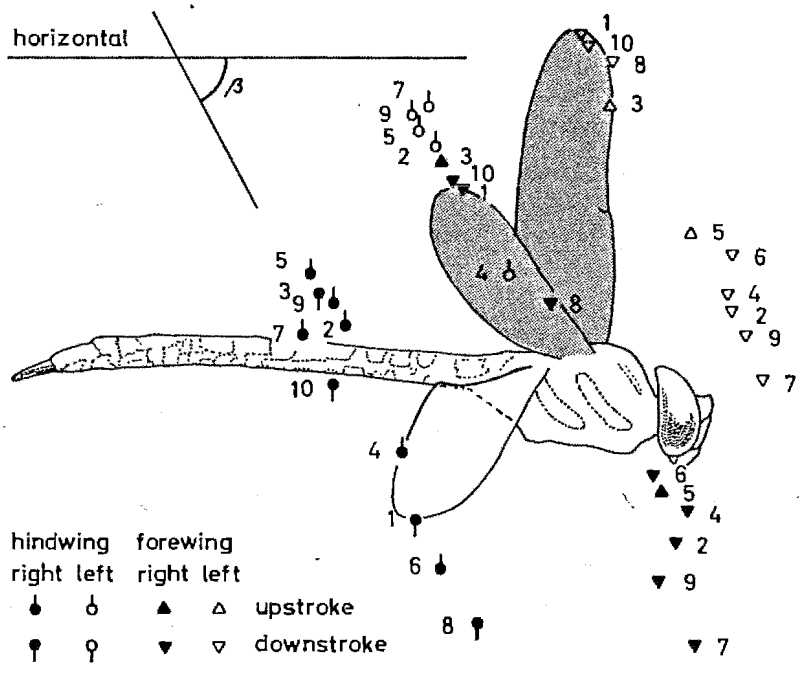
horizontal
β
hindwing right left
forewing right left
upstroke
downstroke

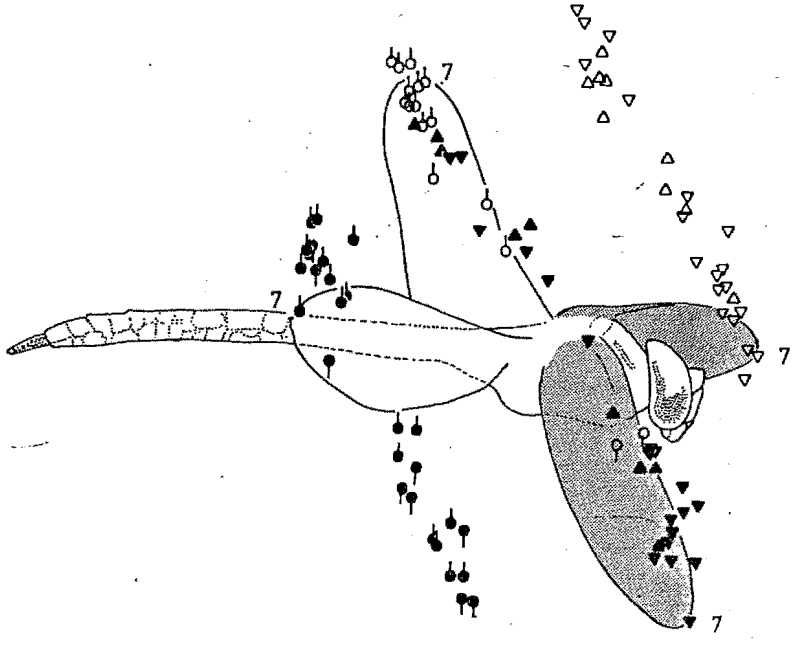

Force Coefficients

The induced velocity was calculated on the assumption that air is accelerated vertically downwards through a 360° disc with the span of the forewings as diameter. The average induced velocity, V_{ind}, at the disc then is 0.62 $msec^{-1}$, while the maximum flapping velocity of the wing tip is 5.34 $msec^{-1}$.

Assuming that the upstroke contributes no upward force, and taking the lift/drag ratio to be 6.5 (see above), an average lift coefficient $\bar{C}_L$ of 6.1 is arrived at.

If the supinated wing works at some angles of attack relative to its morphological dorsal side on the upstroke, then upward forces will be generated also on the upstroke, however smaller than on the downstroke. The resultant force will be tilted more forwards on the upstroke, hence a smaller vertical component. $\bar{C}_L$ then reduces to about 3.5.

When relative wind and force diagrams are constructed, it is found that, averaged over a wing stroke and the whole wings, there must remain a large net horizontal force directed forwards in the cases considered so far (Figure 1). Since this cannot be the case in hovering flight, an alternative assumption is made, namely that the dragonfly is able (by adjustment of angles of attack) to maintain the resultant aerodynamic force on a vertical plane through the long wing-axis (but normal to it) over the whole downstroke. This amounts to assuming a varying lift/drag ratio. Since the upstroke can hardly give any upward force without generating also a horizontal component (cf. Figure 1), the upstroke was again disregarded. Air was assumed to flow through the whole disc as before. Equations (9) and (14) (with F substituted for H) then give an average total force coefficient $(C_L^2 + C_D^2)^{\frac{1}{2}}$ of 4.4. The small differences in coefficients given here and in Norberg (1974) are due to tilts of forces in the transversal plane being allowed for here (equations 12-14).

Figure 3. Free hovering flight of Aeschna juncea. The wing beat frequency is 36 Hz and the exposure frequency 80 Hz. Top. Position of wing tips plotted from 10 consecutive frames (spaced 12.5 msec) representing four wingstrokes. Numbers indicate frame number and are placed in front of the position symbols for the forewings, behind for the hindwings. Wings traced from frame no. 1. Direction of movement of wings is indicated. The forewings (shaded) are in the beginning of the downstroke. The hindwings beat down. Bottom. Position of wing tips plotted from 28 consecutive frames (the 10 of the upper figure inclusive) representing 12 wingstrokes. Wings traced from frame no. 7. The forewings are at bottom of the stroke. The hindwings are supinated and near the end of the upstroke.

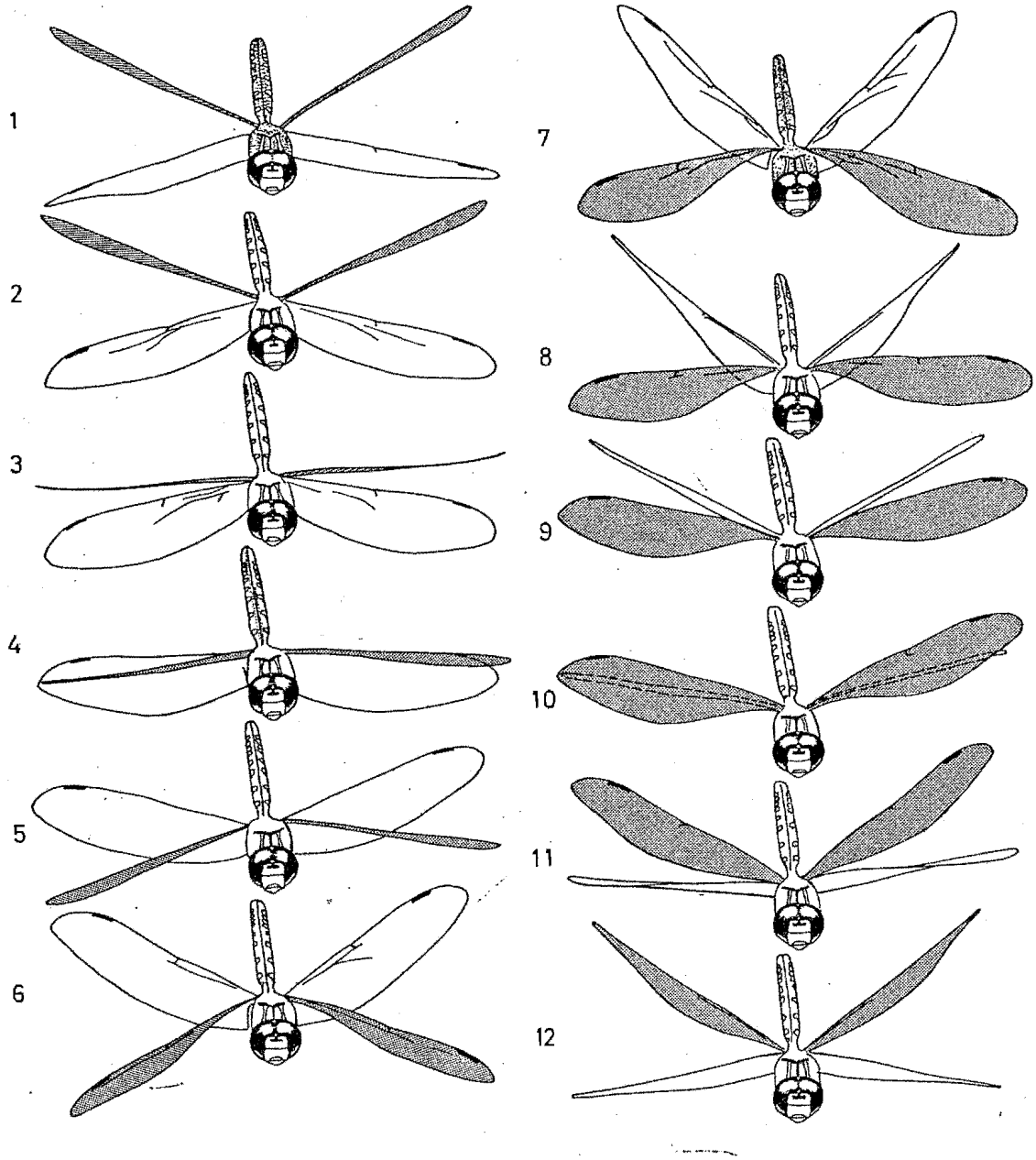

Figure 4. Tracings from a film of Aeschna juncea in free hovering flight. Axis of camera lens normal to the wing stroke plane to within ca. 5°. The wing beat frequency is 37 Hz. The forewings are shaded. The pictures are ordered according to phase and selected from several wing strokes.

(Figures 5-8 show Aeschna juncea in free hovering flight. Photo: R. A. Norberg).

Figure 5. Forewings and hindwings beat down with chord close to the horizontal.

Figure 6. Forewings are in the beginning of the downstroke and hindwings in the beginning of the upstroke.

Figure 7. Forewings and hindwings beat up and are strongly supinated (pitched-up) and twisted.

Figure 8. Forewings at the end of the upstroke, strongly supinated and twisted. Hindwings in the downstroke.

If air is accelerated vertically through smaller areas than the whole disc with wing span as diameter, then the induced velocity becomes larger. But due to the large angle of tilt of the stroke plane, larger values of induced velocity result in lower values of the resultant relative air velocity on the downstroke (cf. Figure 1). Therefore still larger force coefficients would be needed.

DISCUSSION

Force Coefficients

With data from wind tunnel measurements, Jensen (1956) calculated lift coefficients of the forewing of the locust Schistocerca gregaria. Its forewing is rather similar in planform and size to that of Aeschna dragonflies. It also operates at about the same Reynolds number, ca. 2000. With the forewing flat, the maximum coefficient of lift was 1.1. When the forewing was cambered by deflecting its rear part 25°, $C_{L,max}$ rose to 1.3. Schmitz (1960) gave similar values for thin, flat and cambered plates.

From this it is obvious that the force coefficients arrived at here for Aeschna juncea are far too large to be reconcilable with steady-state aerodynamics. This verifies Weis-Fogh's (1973, p. 206) statement. My calculations are based on data for free hovering flight and are carried out under several alternative assumptions. All minimum, average force coefficients arrived at are even considerably larger than Weis-Fogh's.

The most conspicuous reasons why the force coefficients would need to be so high in hovering flight if steady-state aerodynamics did prevail, are (1) the remarkably large angle of tilt of the stroke plane, and (2) the small stroke angle. In these respects dragonflies differ from most other insects.

It seems safe to conclude then, that the upward force needed in hovering flight can be explained with steady-state aerodynamics to only ca. 40% at best. Non-steady-state aerodynamics must be invoked to explain the remaining 60% of the force generated. In forward flight, however, traditional aero-foil function may well predominate, and non-steady phenomena may then be negligible.

Since sufficient force is not generated during the flapping (translatory) phase of the wing stroke in hovering, some other wing movement must be important too. It is shown in this report that pitching wing rotations through large angles occur at top and bottom of the stroke. It is natural then, to assume, as did Weis-Fogh (1973, p. 220), that these wing rotations generate additional forces. The "flip mechanism" outlined by Weis-Fogh consists of a rapid wing rotation about the long wing-axis at the extreme wing positions. The rotation was assumed to be actively controlled from the wing base, and to occur so rapidly that the wing becomes temporarily deformed. There would then be a torsional deformation wave propagating from base to tip. The pterostigma (a pigmented spot at the leading edge far out on the wing) adds mass to the leading edge of the wing of many Odonata and affects wing pitch at the turning points due to inertial effects (Norberg (1972)). It was

assumed by Weis-Fogh to delay the propagation of the torsional wave in hover-flies, Syrphinae. Due to the delay in twist towards the tip, vortex shedding at the tip, and hence loss of useful circulation, would be minimized. Further, chordwise wing deformation was assumed to occur during wing twisting in hover-flies. The rear part of their wings is pliable, and hence the wing profile may become curved temporarily during wing twisting. The rotation at the extreme positions were thought to generate circulation around the wings, and hence lift, already at the beginning of the stroke, without the wing first having to go through some translatory motion to build up circulation.

Because of the low exposure frequency of my films, nothing can be traced directly as to the occurrence of a deformation wave propagating outwards. But wing attitudes in Figures 4:11, 4:12, and 4:1 indicate that supination of the hindwing at bottom of the stroke starts from the wing base. However, at top of the stroke pronation of forewing and hindwing is completed first at the tip, Figures 4:12 and 4:8. This still leaves the possibility of a pitch-down wave propagating outwards, involving only the stiff leading edge and tip parts, but leaving the rear part lagging behind.

The wings beat in essentially the same plane on the downstroke and upstroke. The wing tip path thus is not elliptical as sketched by Weis-Fogh (1973, Figure 23) for the "flip mechanism".

Forewing and hindwing beat out of phase, and interference between them certainly occurs and may cause additional lift. But with one pair of wings the bird Ficedula hypoleuca (Pallas) must attain its high forces in hovering by some other mechanism (U. M. Norberg (1974)). This might be of importance also to dragonflies.

Concluding then, I think that pitching wing rotations at bottom and top of the wing stroke are of great importance for force generation in hovering flight of dragonflies. Non-steady-state aerodynamics are important, but the exact mechanism is still unclear.

The Node

In dragonflies there is a unique morphological arrangement, the node, at the leading edge half way or less from base to tip. Here the leading edge veins bend backwards and cross (Fraser (1948)). The node permits elastic tension of the leading edge, and thus seems to be an adaptation permitting strong wing twistings. It may serve also other functions, for instance that of a shock absorber.

REFERENCES

Fraser, F. C. 1948 A new interpretation of the course of the subcostal vein in the wings of Odonata, with remarks on Zalessky's notation. Proc. R. Ent. Soc. Lond. (A), 23, 44-50.

Hertel, H. 1966 Structure, Form, Movement. Reinhold Publishing Corp., New York.

Jensen, M. 1956 Biology and physics of locust flight. III. The aerodynamics of locust flight. Phil. Trans. R. Soc. B, 239, 511-552.

Norberg, R. Å. 1972 The pterostigma of insect wings an inertial regulator of wing pitch. J. comp. Physiol. 81, 9-22.

Norberg, R. Å. 1974 Hovering flight of the dragonfly Aeschna juncea L. Symp. on Swimming and Flying in Nature, Calif. Institute of Technology. Paper Abstracts, p. 61.

Norberg, U. M. 1974 Hovering flight in the pied flycatcher (Ficedula hypoleuca). Proc. Symposium on Swimming and Flying in Nature, Pasadena, California, July 8-12.

Osborne, M. F. M. 1951 Aerodynamics of flapping flight with application to insects. J. Exp. Biol. 28, 221-245.

Pennycuick, C. J. 1968 A wind-tunnel study of gliding flight in the pigeon Columba livia. J. Exp. Biol. 49, 509-526.

Schmitz, F. W. 1960 Aerodynamik des Flugmodells. Carl Lange Verlag, Duisburg.

Shapiro, J. 1955 Principles of Helicopter Engineering. Temple Press, London.

Sotavalta, O. 1947 The flight-tone (wing stroke frequency) of insects. Acta ent. fenn. 4, 1-117.

Weis-Fogh, T. 1967 Respiration and tracheal ventilation in locusts and other flying insects. J. Exp. Biol. 47, 561-587.

Weis-Fogh, T. 1972 Energetics of hovering flight in hummingbirds and in Drosophila. J. Exp. Biol. 56, 79-104.

Weis-Fogh, T. 1973 Quick estimates of flight fitness in hovering animals including novel mechanisms for lift production. J. Exp. Biol. 59, 169-230.